The calibration model in potassium ion flux non-invasive measurement of plants *in vivo in situ*

CrossMark

Lin Xue [a,b,d], Dong-jie Zhao [a,d], Zi-yang Wang [a,d], Xiao-dong Wang [e], Cheng Wang [e], Lan Huang [a,c,d], Zhong-yi Wang [a,c,d,*]

[a] College of Information and Electrical Engineering, China Agricultural University, Beijing 100083, China
[b] College of Information Technology, Beijing Union University, Beijing 100101, China
[c] Modern Precision Agriculture System Integration Research Key Laboratory of Ministry of Education, Beijing 100083, China
[d] Key Laboratory of Agricultural Information Acquisition Technology (Beijing), Ministry of Agriculture, Beijing 100083, China
[e] National Engineering Research Center for Information Technology in Agriculture, Beijing 100097, China

A B S T R A C T

SIET (Self-referencing Ion Electrode Technique) provides a novel electrophysiological tool which can non-invasively measure the dynamic influxes and effluxes of ions caused by the diffusion along the concentration gradients *in vivo*. However, in this technique ion fluxes are converted to voltage signals using an ion selective microelectrode at a small amplitude of μV, which is easy to be interfered by the ambient noise. Hence, effective solutions to the suppression of noise and calibration of ion flux measurement system are very important for this method. A K^+-selective microelectrode was constructed using liquid ion exchangers (LIX) to investigate ion transport over plant tissue. A standard concentration gradient which simulates plant living cells was produced by an electrode with a certain tip diameter, filled with a solution containing a known K^+ concentration in 100 mmol/L. An ion diffusion simulation model was established. This model evaluated the performance of ion flux measurement system in accuracy and reliability by comparing the consistency of the measured value and the predicted curve. K^+ fluxes were measured within 25 min at each measuring point of distance 10, 20, 30, 40, 50, 80, and 100 μm from the K^+ source, respectively. It can be seen that the K^+ fluxes changes little, which indicates that ion flux measurement system has a reliable stability. The study provides a theoretical basis for a new non-invasive ion flux measurement method creation and a new sensors design.

© 2016 China Agricultural University. Production and hosting by Elsevier B.V. All rights reserved.

1. Introduction

SIET, a novel electrophysiological tool, can non-invasively measure the dynamic influxes and effluxes of ions from living biological samples *in vivo in situ* without damaging the organizational structure. These biological samples include a single cell, cellular level, tissues, and even intact plant. Using this technique various intracellular and extracellular ion concentrations, ion fluxes caused by ion exchange will be easy to measure *in situ*. At present, SIET has been more and more widely used in microbiology, medicine, environmental science, molecular biology, and other fields [1–6] to study the relationship among the transmission process, metabolism and other physiological processes. [7–11].

---

* Corresponding author at: College of Information and Electrical Engineering, China Agricultural University, Beijing 100083, China. Tel./fax: +86 10 62737778.
 E-mail address: wzyhl@cau.edu.cn (Z.-y. Wang).
Peer review under the responsibility of China Agricultural University.

In the ion flux measurement in plants, intracellular and extracellular ion concentrations of plants, and influxes and effluxes of ions from plants are detected by using of ISMEs (Ion Selective Microelectrodes). This kind of biological sensor is pulled from a glass micropipette, filled with pipette electrolyte solution and LIX which converts ion concentration and ion flux to electrical signals. Thus, ion concentration is determined by the electrical signal based on the Nernstian equation.

The voltage gradient over the vibration excursion of the electrode obtained from SIET at μV level which indicates the influxes and effluxes of ions of living plants. It's very easy to be interfered by the ambient noise even submerged. It is important to obtain the weak signal and establish an effective calibration model for non-invasive ion flux measurement which is applied in the plant response to external stimuli. In 1990, Jaffe [12] used a microelectrode with a tip diameter of $\sim$10 μm, filled with high concentration $CaCl_2$ solution, as an artificial standard diffusion source to generate a calcium gradient. The Ca^{2+} concentration and the Ca^{2+} flux were measured along the calcium gradient by the ion flux measurement system. The accuracy, sensitivity and repeatability of the measurement system then were detected by comparing the measurement and theoretical value. Doughty [13] also tested his ion flux measurement using the same method by the detection of Cl^- at different distance of the Cl^- standard source with a certain Cl^- concentration. This method using an artificial standard diffusion source to generate a stable gradient is of high accuracy and easy to repeat. These authors put forward a relational model between the voltage difference signal of microelectrode and the distance from the standard source, but did not take into account the influence of time on their model.

K^+ is one of the main nutrient elements in plants, which involves in the most physiological processes [14] and plays important roles in the process of the electrical signal change when plants respond to external stimuli [15–17]. Matsuoka [15] analyzed the K^+ response to CO_2 stress in *Tradescantia virginiana* L. in the vacuole in leaf cells. Chen [16] measured leaf mesophyll K^+, H^+, and Ca^{2+} fluxes involved in drought-induced decrease in photosynthesis and stomatal closure in soybean. Pottosin [17] studied the difference of the extent of potentiation of the ROS-induced K^+ efflux by polyamines in the salt-sensitive and salt-tolerant barley varieties.

This paper establishes an improved calibration model for K^+ flux measurement system. It not only analyzes relationship between the voltage difference signal of microelectrode and the distance from the standard source, but also analyzes relationship between the voltage difference signal of microelectrode and time. After calibration by this improved model the ion flux measurement system is applied in the measurement of the K^+ flux of maize seedling root.

2.　Ion flux measurement system and principle

The ion flux measurement system includes an ion selective microelectrode, a reference electrode, a high impedance microelectrode amplifier, an electric micro manipulator, a faraday cage, an anti-vibration platform, a microscope, and a computer with relevant software as shown in Fig. 1. The Faraday cage is a container made of conductive material that shields external electromagnetic interference. The anti-vibration platform reduces the effect caused by mechanical vibrations. And the voltage signal measured by a microelectrode will be magnified by a high impedance microelectrode amplifier ($>10^{13}$ Ω), and then output to a computer with ion flux acquisition and calculation software for real-time recording.

An ion selective microelectrode consists of glass microelectrode, Ag/AgCl wire, pipette electrolyte solution and liquid ion exchanger (see Fig. 2) [18]. The relationship of the voltage output E of the microelectrode and the ion concentration C is described using the Nernstian equation Eq. (1):

$$E = k \pm s \ \lg C \tag{1}$$

where E is the measured voltage between microelectrode and reference electrode (mV); C is the ion concentration (mol/L); s is Nernstian slope (mV/dec); k is Nernstian intercept (mV). For a monovalent cation, the theoretical value of Nernstian slope is 59.16 mV/dec at 25 °C. In practice, s is determined by the calibration using two different known concentration. According to the Nernstian equation, there is a significant linear correlation between the ISME's voltage and logarithm of the ion concentration. Then the ion concentration can be calculated based on the ISME's voltage measured.
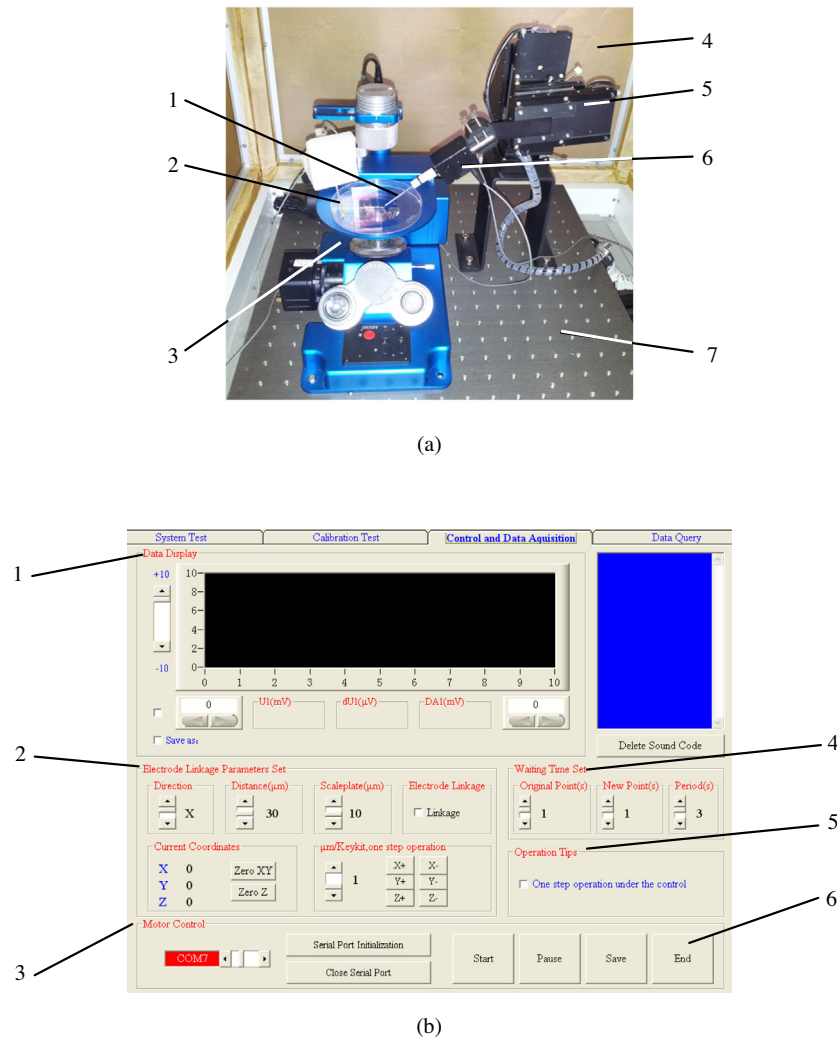
The ion selective microelectrode is positioned at a small distance (5–10 μm) of the cell, tissue, or organ as shown in Fig. 3. A motor-driven manipulator is used to move the ISME at 2 points over a known distance Δx (10–30 μm, and less than 30 μm) at a low frequency, to measure the voltage signals V_1 and V_2 at each point. Thus the concentration difference ΔC between these 2 points will be calculated by the microelectrode voltage/concentration calibration curve. The ISME moves at a low frequency (routinely no more than 0.5 Hz), which does not affect the distribution of the ion concentration gradient [12,14]. Then the specific ion flux in a certain direction will be obtained from Fick's law:

$$J = D \times \Delta C/\Delta x \tag{2}$$

where J is the ion flux in the x direction ($pmol/(cm^2 \ s)$); D is ion/molecule diffusion constant (cm^2/s); $\Delta C/\Delta x$ is ion concentration gradient ($pmol/cm^4$).

3.　Materials and methods

K^+ is one of most important ions with a high concentration at 100–200 mmol/L in the higher plant cells, while it is generally dozens of times more than that of extracellular. In fact, K^+ concentration of the environment plants grow in usually maintains 1–10 mmol/L, and even as low as 0.3–0.5 mmol/L [19]. Hence, a plant living cell can be equivalent to a time-continuous point source with a constant K^+ concentration. To determine the performance of ion flux measurement system, we used a microelectrode filled a certain known K^+ concentration as an artificial point source to generate a range of known, steady K^+ concentration gradients without significant voltage gradients.

(a)

(b)

Fig. 1 – Configuration of the ion flux measurement system. (a) Ion flux measurement hardware. 1. Ion selective microelectrode; 2. Reference electrode; 3. Microscope; 4. Faraday cage; 5. Electric micro manipulator; 6. High impedance microelectrode amplifier; 7. Anti-vibration platform. (b) Ion flux acquisition and calculation software. 1. Ion flux measured display with the U1 (mV) and dU1 (μV) as the voltage E of microelectrode and the voltage difference ΔV between two positions Δx, separately; 2. Control panel of the electric micro manipulator to change the microelectrode's position in μm with buttons "X+", "X−", "Y+", "Y−", "Z+", "Z−", and the microelectrode moving direction and distance; 3. Switch of the electric micro manipulator; 4. Waiting time set of the microelectrode after moving to original or new point; 5. Checkbox to allow one step operation of the electric micro manipulator or not; 6. On–off control buttons. Note: The computer is not shown here.
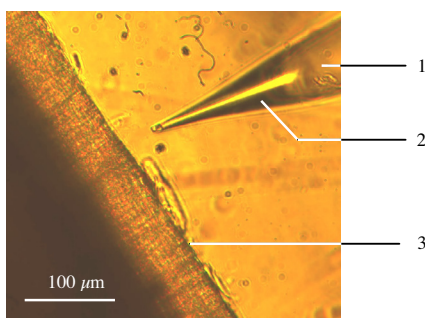
Fig. 2 – Ion selective microelectrode. 1. Glass microelectrode; 2. Liquid ion exchanger; 3. Maize root. Note: Ag/AgCl wire is not shown here.

3.1. Fabrication of K$^+$-ISME

Microelectrodes were pulled from filamented borosilicate glass capillaries using a horizontal puller (Flaming/Brown P97 puller, Sutter Instruments, USA), with a diameter of ~5 μm. The microelectrodes need to be silanized with dimethyldichlorosilane (Fluka 40136, Fluka Chemical Ronkonkoma, NY) in the clean-room before use to prevent rapid losing of liquid ion exchanger which was described by Xue (2013) detailly [20]. Before or after silanization, the microelectrodes were heated at 200 °C for 1 h to ensure dryness or remove the excess dimethyldichlorosilane [21]. Then microelectrodes were back-filled with 100 mmol/L KCl solution, and front-filled with ~180 μm length column of liquid ion exchanger of potassium (Potassium ionophore I – cocktail A
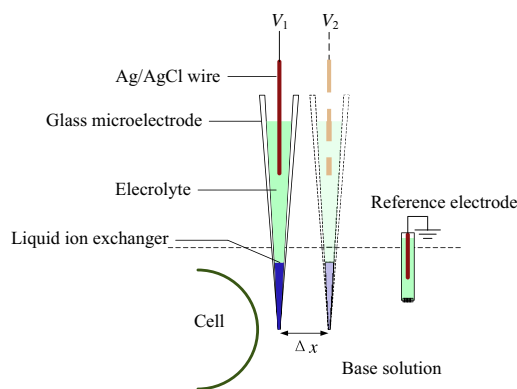
Fig. 3 – Ion flux measurement principle. Note: V_1, V_2 are measured voltages for different gradients at 2 positions in distance Δx using the ion selective microelectrode, respectively, mV; Δx is the distance between 2 positions where the ion selective microelectrode vibrated, μm.

(60031), Sigma, USA). Electrical contact is established by inserting an Ag/AgCl wire into the back of microelectrode.

3.2. Calibration of K^+-ISME

The Nernstian properties of each ISME were tested by measuring the microelectrode voltage output in 1, 10 and 100 mmol/L KCl solution, respectively. A regression of the voltages (mV) against logarithm of the K^+ concentrations needs to yield a straight line. ISMEs were discarded if the slope of the regression line is less than 53 mV/dec.

3.3. Measurement of ion flux of an ion gradient source

As an artificial K^+ source a filamented microelectrode (without silanization) with a tip diameter of 5 μm, filled with 100 mmol/L KCl plus 1 mmol/L $CaCl_2$ was placed in a small petri dish containing 1 mmol/L KCl and 100 mmol/L $CaCl_2$ and waited about 1 h for a steady state to be established with a range of known, steady K^+ concentration gradient. Counter diffusion of Ca^{2+} minimized osmotic water flow as well as diffusion potentials. And the tip of the ion source microelectrode was placed relatively close to the bottom of the dish.

The steady concentration C at a distance x from the ion source was given by:

$$C = C_B + K/x \tag{3}$$

where C_B was the K^+ background concentration (μmol/cm^3); K was an empirical constant that depended on characteristics of both the artificial source and base solution; x was the distance between the K^+ source and K^+-ISME (μm), as shown in Fig. 4. The concentration C could be easily measured as a function of x by using a stationary K^+-ISME. Substituting C and x into Eq. (3), the C_B and K would be obtained.

A prediction for the voltage difference ΔV as a function of distance x from the K^+ source could be calculated using the equation, which was described by Kühtreiber and Jaffe (1990) in detail:

$$\Delta V = \frac{s}{2.3} \frac{-K \cdot \Delta x}{C_B x^2 + Kx} \tag{4}$$
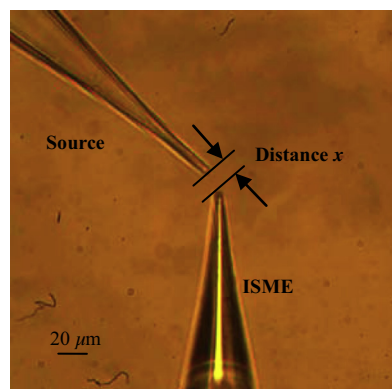
Fig. 4 – Diagram illustrating of standard K^+ gradients measurement.

where s was the Nernstian slope (mV) of the ISME; Δx was vibration amplitude (μm).

The K^+ concentration difference would be obtained by the equation:

$$\Delta C \approx (2.3(\Delta V \cdot C_B))/s \tag{5}$$

Then the ion flux J at the known distance x from the K^+ source would be obtained from Eqs. (2)–(5).

4. Results and discussion

### 4.1. Result of K^+-ISME calibration

At 25 °C, the K^+-ISME voltages was −23.44 mV, 32.23 mV and 84.96 mV when placed in a series of standard KCl solutions (1, 10 and 100 mmol/L), respectively. Substituting into Eq. (3), the result s was calculated to be 54.20 mV/dec with a conversion rate of 91.62% compared with the theoretical value 59.16 mV/dec which met the requirement of ISMEs. Whereby a voltage/concentration calibration curve was shown in Fig. 5.

4.2. Result of standard K^+ concentration gradients measurement

The K^+-ISME steady voltages at the positions of 10, 20, 30, 40, 50, 80, and 100 μm far from the K^+ source were measured, respectively. Converting voltages to ion concentrations using the Nernstian relationship in Fig. 5, the linear relationship between K^+ concentration and 1/distance was obtained, fitted with a linear regression in the Eq. (6), as shown in Fig. 6.

$$y = 0.0004885002x + 1.0132731389 \tag{6}$$
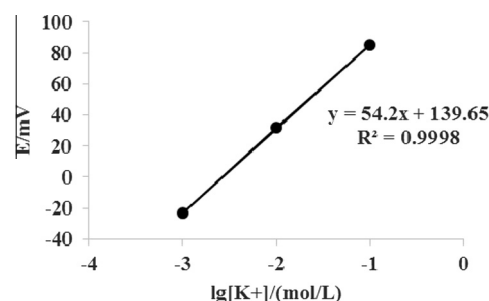
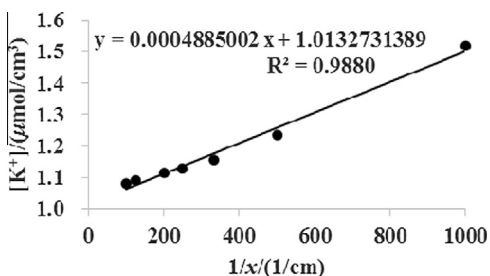**Fig. 5 – Voltage/concentration calibration curve.**

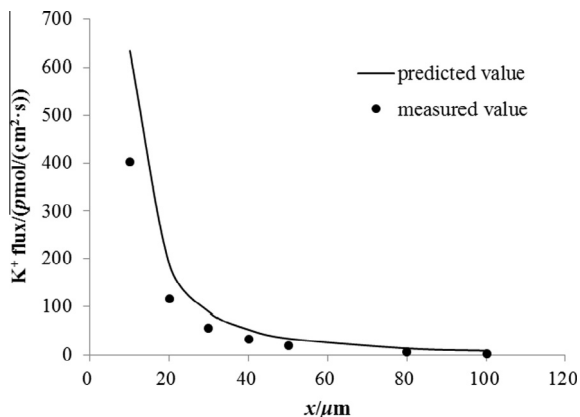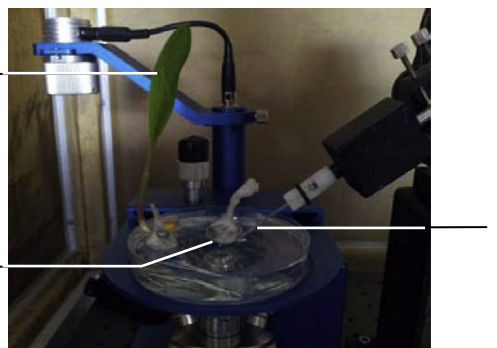Fig. 6 – K⁺ concentration against 1/distance linear relation.

Fig. 9 – Physical map of measurement of K⁺ flux across intact root of maize. 1. Maize leaf which was the stimulation point; 2. Maize root which was recording region; 3. K⁺-ISME.

Fig. 7 – K⁺ fluxes measured at a set of known positions (vibration amplitude Δx is 10 μm, vibration frequency is 0.33 Hz).

By Eqs. (3) and (6), C_B was calculated as 1.0132731389 mmol/L, and K was 0.0004885002 μmol/cm^2.

A K⁺-ISME was repeatedly vibrated along the direction away from the K⁺ source with amplitude of 10 μm (vibrating frequency: 0.33 Hz) at a set of known positions x of 10, 20, 30, 40, 50, 80, and 100 μm far from the K⁺ source, respectively. Thus the voltage difference of K⁺-ISME at each position would be measured, and the K⁺ flux would be calculated, as shown in Fig. 7.

In Fig. 7, the solid line represents a prediction of the K⁺ flux ($pmol/(cm^2\,s)$) self-referenced over a 10 μm excursion, which was calculated from Eqs. (2)–(5), where $s = 54.20$ mV/dec, $C_B = 1.0132731389$ mmol/L, $K = 0.0004885002$ μmol/cm^2, $\Delta x = 10$ μm, and x = distance from source (cm). According to Fig. 7, the actual measured K⁺ flux ($pmol/(cm^2\,s)$, represented by the solid circles) followed closely the predicted curve, which testified the ion flux measurement system capable of accurately and reliably to measure the dynamic influxes and effluxes of ions of plants.

Next, we studied the K⁺ fluxes changing with time at a certain distance from the ion standard source, as shown in Fig. 8. Fig. 8 shows the K⁺ fluxes changing in 25 min at each measuring point of distance 10, 20, 30, 40, 50, 80, and 100 μm from the ion source, respectively. It can be seen that the K⁺ fluxes changes little at each point, which indicates that ion flux measurement system has a reliable stability.

4.3. Measurement of K⁺ flux across intact root of maize

In this work, a 5–7 days old maize root was fixed into a small petri dish containing test solution (0.1 mmol/L KCl, 2.0 mmol/
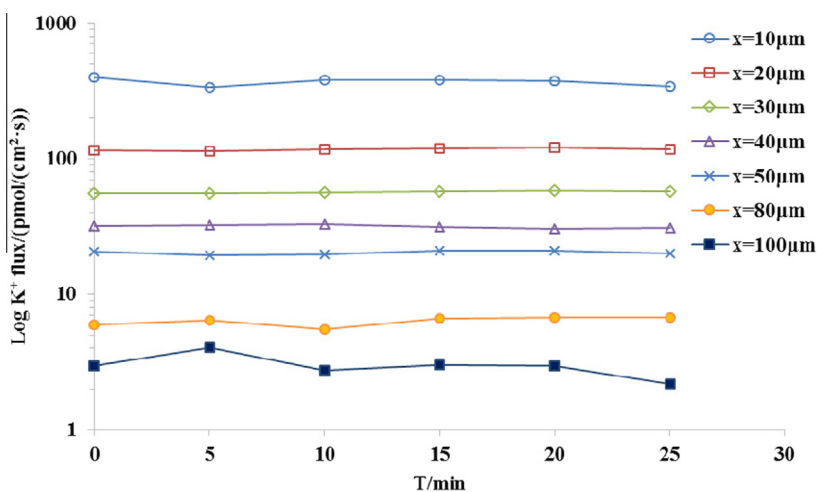

Fig. 8 – K⁺ flux measured at each known position (vibration amplitude Δx is 10 μm, vibration frequency is 0.33 Hz).
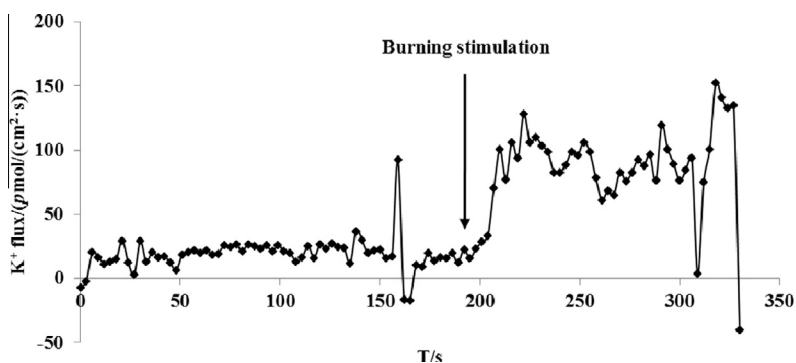
Fig. 10 – K⁺ flux of maize root by burning stimulation.

L CaCl$_2$, 1.0 mmol/L MgCl$_2$, 1 mmol/L MES, and 0.2 mmol/L Na$_2$SO$_4$; pH adjusted to 6.0 with NaOH) and waited about 0.5 h before measurement [22]. The maize leaves and stem were out of the solution. Thermal stimulation as a stress was applied to the maize leaf, which the distance between the stimulation point and recording region of the root was 8 cm. Stimulation was performed by passing a flaming match under the leaf tip for 2 s in an area measuring approximately 1.5 cm^2. The K⁺-ISME was positioned 10 μm above the root surface, which excursion distance was 10 μm and vibrating frequency was 0.33 Hz. The measurement was performed in the zone 100 μm from the root apex. The physical map of voltage differences measurement was shown in Fig. 9.

In Fig. 10, the measured voltage difference ΔV which indicated the net K⁺ flux of maize seeding root responsed to burning stimulation using the ion flux measurement system. After a burning stimulation for 2 s in the maize leaf, which 8 cm far from the measurement position, the K⁺ flux obviously raised from $\sim$25 $pmol$/(cm^2 s) (normal level) up to $\sim$100 $pmol$/(cm^2 s) and last for more than 2 min. The data preliminarily revealed K⁺ efflux triggered by thermal stress which impacted on the K⁺ transport. In addition, localized measurements of specific ion flux of plant roots, with fine spatial and temporal resolution, are now probably a more suitable method than other techniques to elucidate the function and regulation of transporters [23–24]. Our findings in the present work are also consistent with the previous reports.

5.   Conclusion

Based on the distribution of ions inside and outside of plant living cells, taking K⁺ for example, the ion source equivalent form of single plant living cell and the spatial and temporal distribution of ion diffusion were discussed. An artificial stable K⁺ source used to generate gradient which simulated plant living cells was achieved by a microelectrode with a certain tip diameter, filling of solution containing a known K⁺ concentration. A calibration model was established and evaluated the performance of ion flux measurement system in accuracy and reliability.

The results indicated that the measured values were consistent with the predicted ones. The study provides a theoretical basis for a non-invasive ion flux measurement method creation and new sensors design. Hence, the SIET maybe

becomes a potential useful tool to obtain ion transport of plants under stress.

REFERENCES

[1] Sun, Chen SL, Dai SX, Wang RG, Li NY, Shen X, et al. NaCl-induced alternations of cellular and tissue ion fluxes in roots of salt-resistant and salt-sensitive poplar species. Plant Physiol 2009;149(2):1141–53.

[2] Javier I, Lívia N, Ágnes V, István B, Géza N, Ricardo MS. Scanning electrochemical microscopy for the investigation of corrosion processes: measurement of Zn^{2+} spatial distribution with ion selective microelectrodes. Electrochim Acta 2012;59:398–403.

[3] Yue YS, Zhang MC, Zhang JC, Duan LS, Li ZH. SOS1 gene overexpression increased salt tolerance in transgenic tobacco by maintaining a higher K⁺/Na⁺ ratio. J Plant Physiol 2012;169:255–61.

[4] Li LZ, Liu XL, Peijnenburg WJGM, Zhao JM, Chen XB, Yu JB, et al. Pathways of cadmium fluxes in the root of the halophyte *Suaeda salsa*. Ecotoxicol Environ Saf 2012;75(1):1–7.

[5] Teakle NL, Bazihizina N, Shabala S, Colmer TD, Barrett-Lennard EG, Rodrigo-Moreno A, et al. Differential tolerance to combined salinity and O$_2$ deficiency in the halophytic grasses *Puccinellia ciliata* and *Thinopyrum ponticum*: the importance of K⁺ retention in roots. Environ Exp Bot 2013;87:69–78.

[6] Javier I, Lívia N, István B, Ricardo MS, Géza N. Potentiometric scanning electrochemical microscopy for the local characterization of the electrochemical behaviour of magnesium-based materials. Electrochim Acta 2013;87:283–93.

[7] Smith PJS. Non-invasive ion probes – tools for measuring transmembrane ion flux. Nature 1995;378(6557):645–6.

[8] McLamore ES, Porterfield DM. Non-invasive tools for measuring metabolism and biophysical analyte transport: self-referencing physiological sensing. Chem Soc Rev 2011;40 (11):5308–20.

[9] Levin M. Molecular bioelectricity in developmental biology: new tools and recent discoveries. BioEssays 2012;34 (3):205–17.

[10] Tegg RS, Shabala SN, Cuin TA, et al. Mechanisms of thaxtomin A-induced root toxicity revealed by a thaxtomin A sensitive *Arabidopsis* mutant (*ucu2-2/gi-2*). Plant Cell Rep 2016;35(2):347–56.

[11] Muralidhar A, Shabala L, Broady P, et al. Mechanisms underlying turgor regulation in the estuarine alga *Vaucheria erythrospora* (Xanthophyceae) exposed to hyperosmotic shock. Plant Cell Environ 2015;38(8):1514–27.

[12] Kühtreiber WM, Jaffe LF. Detection of extracellular calcium gradients with a calcium-specific vibrating electrode. J Cell Biol 1990;110(5):1565–73.

[13] Doughty JM, Langton PD. Measurement of chloride flux associated with the myogenic response in rat cerebral arteries. J Physiol 2001;534(Supp. 3):753–61.

[14] Demidchik V. Mechanisms and physiological roles of K^+ efflux from root cells. J Plant Physiol 2014;171(9):696–707.

[15] Saito M, Matsuoka H. Application of a multifunctional microelectrode to the in vivo analysis of the K^+ response to CO_2 stress. Bioelectrochem Bioenergy 1996;39(1):115–8.

[16] Mak M, Babla M, Xu SC, et al. Leaf mesophyll K^+, H^+ and Ca^{2+} fluxes are involved in drought-induced decrease in photosynthesis and stomatal closure in soybean. Environ Exp Bot 2014;98(98):1–12.

[17] Velarde-Buendía AM, Shabala S, Cvikrova M, et al. Salt-sensitive and salt-tolerant barley varieties differ in the extent of potentiation of the ROS-induced K^+ efflux by polyamines. Plant Physiol Biochem 2012;61:18–23.

[18] Yan XF, Wang ZY, Huang L, Wang C, Hou RF, Xu ZL, et al. Research progress on electrical signals in higher plants. Prog Nat Sci 2009;19(5):531–41.

[19] Qiu QS. Research progress on the plasma membrane potassium ion transporters. Chin Bull Bot 2000;17(1):34–8.

[20] Xue L, Zhao DJ, Hou PC, Wang XD, Wang Y, Wang C, et al. Research of potassium ion selective microelectrode's fabrication and performance test in SIET applications. Trans Chin Soc Agric Eng 2013;29(16):182–9.

[21] Ikeda R, Nakaya K, Yamazaki MT, et al. Effect of vestibular labyrinth destruction on endocochlear potential and potassium concentration of the cochlea. Hear Res 2010;265(1–2):90–5.

[22] Shabala SN, Lew RR. Turgor regulation in osmotically stressed Arabidopsis epidermal root cells. Direct support for the role of inorganic ion uptake as revealed by concurrent flux and cell turgor measurements. Plant Physiol 2002;129:290–9.

[23] Newman IA. Ion transport in roots: measurement of fluxes using ion-selective microelectrodes to characterize transporter function. Plant Cell Environ 2001;24:1–14.

[24] Shabala S, Shabala L, Bose J, Cuin T, Newman I. Ion flux measurements using the MIFE technique. In: Maathuis FJM, editor. Plant mineral nutrients: methods and protocols. Methods in molecular biology. United States of America: Humana Press; 2013. p. 171–83.